ISBN: 978-3-95450-247-9 ISSN: 2673-5490 doi: 10.18429/JACoW-IPAC2024-MOPG29

NUMERICAL SIMULATIONS OF HARMONIC LASING AT SASE2 BEAMLINE OF European XFEL

C. Lechner*, S. Casalbuoni, G. Geloni, European XFEL, Schenefeld, Germany
E. Schneidmiller, Deutsches Elektronen-Synchrotron DESY, Hamburg, Germany

Abstract

In high-gain free-electron lasers (FELs) with planar undulators it is possible (in the linear regime) to independently amplify at the fundamental and at odd harmonics, a process referred to as Harmonic Lasing (HL). For the HL process preservation of the quality of the incoming high-brightness electron beam is essential. This requires suppression of the lasing at the fundamental, which can be achieved using several methods such as special phase shifter set points and attenuation of the fundamental radiation using intra-undulator optical high-pass filters. The European XFEL variable-gap undulator beamline SASE2 features two intra-undulator stations combining a magnetic chicane and the possibility to insert a thin diamond crystal onto the optical axis of the beamline. While installed for the operation in hard x-ray self seeding (HXRSS) mode, this hardware is well-suited for HL experiments at a low electron beam energy corresponding to a fundamental photon energy of about 2 keV. In this contribution we present numerical simulations of third-harmonic lasing at this working point.

INTRODUCTION

European XFEL [1] plans to upgrade the hard x-ray permanent magnet undulator (PMU) beamline SASE2 with an superconducting undulator (SCU) afterburner [2, 3] installed directly at the exit of the already operating SASE2. This upgrade will enable extending the photon energy range beyond the current nominal maximum of 25 keV.

In free-electron lasers (FELs) with planar undulators, light fields at the fundamental and at odd harmonics can be amplified independently (in the linear regime), a process referred to as harmonic lasing (HL) [4–6]. In the x-ray wavelength range, harmonic lasing was demonstrated at a wavelength of 1 nm at PAL XFEL [7] and at a photon energy of 4.5 keV at the SASE3 beamline of European XFEL [8]. Attractive properties of harmonic lasing include the spectral brightness of the harmonic at saturation being comparable to that of the fundamental [8], therefore HL at the third harmonic constitutes a candidate for the generation of microbunches in SASE2 undulator beamline before the electron bunch enters the SCU. The hardware currently installed at SASE2 beamline of European XFEL enables two techniques to disrupt fundamental FEL gain: (i) sequences of special phase shifter setpoints and (ii) spectral filtering. This enables initial harmonic lasing experiments at longer x-ray wavelengths to prepare harmonic-lasing-driven operation of the SCU beamline.

* christoph.lechner@xfel.eu

HARMONIC LASING AT SASE2

Selection of Operating Point

For the operation of hard x-ray self seeding (HXRSS) [9, 10], the SASE2 undulator beamline at European XFEL features two intra-undulator stations combining a magnetic chicane with the possibility to insert and precisely position diamond crystals on the optical axis of the undulator beamline. In this work, we consider using these crystals (thickness d) in the second HXRSS monochromator as optical high-pass filters and with the pitch angle ϕ the effective material thickness $d_{\mathrm{eff}} = d/\sin\phi$ can be adjusted to some extent (the smallest possible pitch angle is about 30°). From the Lambert-Beer law, $T = \exp(-\mu d_{\mathrm{eff}})$, with μ being the attenuation coefficient of the filter material diamond at the photon energy of interest, we see that the x-ray transmission T of the crystal can thus be adjusted to some extent. The applicability of this filtering scheme requires an optical filter combining significant attenuation at the fundamental with reasonable transmission at the third harmonic. From these requirements and the currently installed diamond crystal (d = 105 µm, density of diamond: ρ = 3.5 g cm^{-3}) follows an electron beam energy of 8.5 GeV and a photon energy of 2.3 keV (corresponding to the SASE2 undulators set to K = 3.59). Filter transmission values were computed for the fundamental photon energy of 2.3 keV and selected pitch angles using data from Ref. [11], the data is compiled in Table 1. For the selected photon energies, the filter element attenuates the fundamental by several orders of magnitude while only mildly attenuating the third harmonic.

Table 1: Filter Transmission Data for Diamond Crystal with Thickness d = 105 µm for Various Pitch Angles (fundamental photon energy 2.3 keV)

pitch angle	T_1	T_3
90° (normal incidence)	$6.4 \cdot 10^{-4}$	0.77
53°	$1.0 \cdot 10^{-4}$	0.73
45°	$3.0 \cdot 10^{-5}$	0.70
30°	$4.1 \cdot 10^{-7}$	0.60

FEL Simulations

The simulations were performed using version 4 of the FEL simulation code "Genesis 1.3" [12–14] in "one4one" simulation mode (tracking actual electrons instead of macroparticles). The electron bunch is generated using the initial parameters listed in Table 2. It is guided around the crystal by a chicane with a minimum required delay of about 15 fs, washing out any microbunching since $k_1\sigma_\delta R_{56} \gg 1$

ISBN: 978-3-95450-247-9 ISSN: 2673-5490 doi: 10.18429/JACoW-IPAC2024-MOPG29

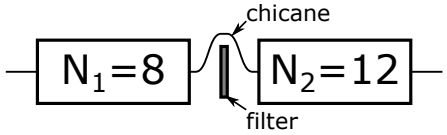

Figure 1: Schematic layout of the system under study.

Table 2: Simulation Parameters

Parameter	Value
electron beam energy	8.5 GeV
initial energy spread	1.5 MeV
bunch peak current	2.5 kA
bunch length	12 µm
normalized emittance	0.4 mm mrad
$\langle\beta_x\rangle/\langle\beta_y\rangle$	32.3 m / 26.5 m
filter transmissions	$T_1 = 1.0 \cdot 10^{-4}$
	$T_3 = 0.73$

(here $k_1 = 2\pi/\lambda_1$ is the wavenumber of the fundamental wavelength and $\sigma_\delta = \sigma_\gamma/\gamma_0$ is the relative energy spread). In the simulation model with a flat-top electron bunch, this delay reduces the fraction of the photon pulse that is in temporal overlap with electrons along the entire beamline and therefore also influences the choice of the length of the electron bunch and the length of the simulation window. To reduce the complexity of the FEL simulations without loss of accuracy, wakefields in the electron beamline and energy losses due to spontaneous radiation are not taken into account (the growth of energy spread due to spont. radiation is included) and the undulator is untapered. One additional simplification in these initial simulations is the assumption that the chicane is not installed in an 'empty' (i.e. without undulator) half-period of the FODO lattice but would fit into a standard intersection. Because of the different propagation properties of the fundamental and third-harmonic light fields, adjustments of the parameters may be required once this is implemented into the simulation model.

Figure 1 shows the schematic layout of the beamline which corresponds to the undulator configuration of SASE2 around the second HXRSS monochromator. Up to eight 5-meter-long variable-gap undulator segments can be used before and up to 19 after the HXRSS monochromator, respectively.

At the studied operating point the FEL gain length is high. In this case standard FEL codes do not accurately simulate the transverse radiation distribution, especially at large angles, resulting in an incoherent "pedestal" in the transverse radiation distribution. While not influencing the accuracy of the results, this simulation effect distorts the apparent pulse energy growth at the beginning of the amplification process (solid lines in Fig. 2a). To address this issue, the light fields are analyzed in the far field [15], taking only small-angle energy contributions into account, where the FEL radiation dominates. For additional information, the reader is referred to Ref. [3]. This analysis is not required for the generated third-harmonic photon pulse close to the end of the undulator beamline.

In Fig. 2 we show the evolution of selected parameters along the undulator beamline. In Fig. 2a, the evolution of the photon pulse energy at the fundamental (2.3 keV, indi-cated in blue) and at the third harmonic (6.9 keV, indicated in red) is plotted. Pulse energies computed using the far-field analysis described above are indicated as dashed lines (aper-ture half-angles of about 3.6 µrad for 2.3 keV and 1.2 µrad for 6.9 keV, respectively) and the total pulse energies are indicated as solid lines.

The optical high-pass filter attenuates the fundamental light field by four orders of magnitude while the chicane washes out the microbunching (Fig. 2b). In the undulators after the chicane, lasing at the third harmonic is initiated by the mildly attenuated light field generated upstream of the filter.

Figure 2 shows the evolution along 12 undulator segments after the high-pass filter. At the end of this beamline, the third-harmonic photon pulse energy is 73 µJ and the pulse energy of the fundamental is 15 µJ. After about 8 undu-lator segments, the growth rate of the fundamental lasing begins to increase, resulting in a reduction of the contrast U_3/U_1 of photon pulse energies for the remaining undulator beamline. Depending on the application one could therefore operate with only eight undulators after the filter/chicane combination.

In Fig. 3, the longitudinal profiles of selected photon pulse and electron bunch properties are plotted for the position eight undulators after the filter/chicane combination ($z = 96.3$ m in Fig. 2). Figure 3a shows the flat-top current profile (black dashed) and the longitudinal power profiles of both the third harmonic (red) and the fundamental (blue). The third-harmonic peak power is in the gigawatt range, with the total third-harmonic photon pulse energy being about 30 µJ. In the trailing parts of the electron bunch there is no significant lasing, which is the result of the photon fields advancing in the chicane with respect to the electron bunch. The region of the bunch with third-harmonic lasing exhibits also significant third-harmonic bunching (Fig. 3b), therefore an attractive option to further amplify only the third-harmonic radiation may be to tune the fundamental of subsequent SASE2 undulator segments to the 6.9-keV photon energy (this would resemble the SCU afterburner operation scheme studied in Ref. [3]).

In this work, the phase shifters situated between the undulator segments were adjusted by repeating the special setpoint pattern $2\pi/3$; $2\pi/3$; $4\pi/3$; $4\pi/3$ (in Genesis notation). We note that there exist many patterns composed from the values $2\pi/3$, $4\pi/3$, and 0 and their performance has to be assessed numerically.

SUMMARY

We performed numerical FEL simulations of harmonic lasing at the photon energy of 6.9 keV (with the fundamental photon energy being 2.3 keV) using the hardware already

ISBN: 978-3-95450-247-9 ISSN: 2673-5490 doi: 10.18429/JACoW-IPAC2024-MOPG29

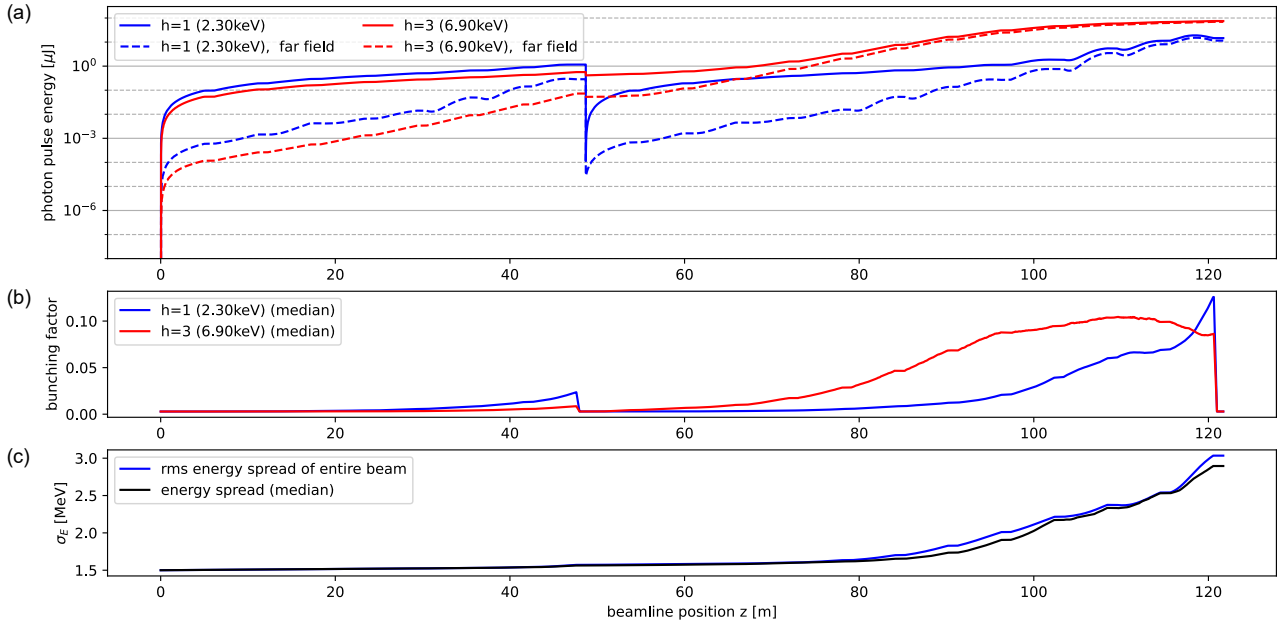

Figure 2: Evolution of selected parameters along the system under study, comprising eight SASE2 undulators, followed by the filter/chicane combination, followed by 12 SASE2 undulators. (a) Photon pulse energy at the fundamental (blue) and at the third harmonic (red), respectively. The dashed lines indicate the result of the far-field analysis described in the text while the total pulse energy is indicated as solid lines. (b) Bunching factors along the beamline. (c) Evolution of slice energy spread along the beamline.

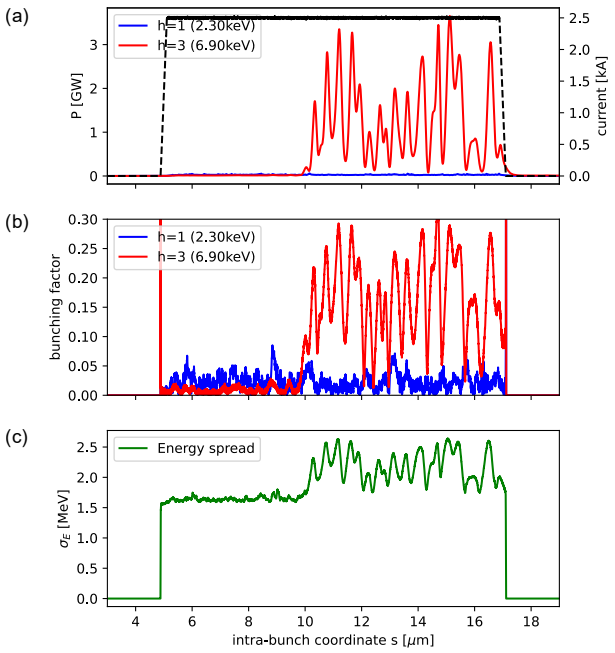

Figure 3: Longitudinal profiles after propagating along eight undulators following the filter/chicane combination. Head of the bunch to the right. (a) Current profile of electron bunch (black dashed) and power profiles of third harmonic (red) and fundamental (blue); (b) bunching factors for third harmonic (red) and fundamental (blue); (c) longitudinal profile of slice energy spread.

in operation at the SASE2 beamline of European XFEL. The combination of special phase shifter setpoints and the diamond crystal installed in the HXRSS monochromator chamber suppresses fundamental lasing and preserves the quality of the high-quality electron bunch. Eight undulators downstream of the filter/chicane combination, the photon pulses generated by harmonic lasing exhibit gigawatt-range peak power (Fig. 3a).

Harmonic lasing is a promising candidate to drive emission from the planned upgrade of SASE2 beamline with an SCU afterburner. For further studies of harmonic lasing, simulations of an operating point with a fundamental photon energy between 2.3 keV and 16.7 keV (see Ref. [3]) could be performed (including considerations into high-pass filtering options).

ACKNOWLEDGEMENTS

The numerical simulations were supported by the "MAXWELL" computational resources operated at Deutsches Elektronen-Synchrotron DESY, Hamburg, Germany.

REFERENCES

[1] W. Decking *et al.*, "A MHz-repetition-rate hard X-ray free-electron laser driven by a superconducting linear accelerator," *Nat. Photonics*, vol. 14, pp. 391–397, 2020. doi:10.1038/s41566-020-0607-z

ISBN: 978-3-95450-247-9 ISSN: 2673-5490 doi: 10.18429/JACoW-IPAC2024-MOPG29

[2] S. Casalbuoni *et al.*, "Superconducting undulator activities at the European X-ray Free-Electron Laser Facility," *Front. Phys.*, vol. 11, p. 1 204 073, 2023. doi:10.3389/fphy.2023.1204073

[3] C. Lechner *et al.*, "Numerical simulation studies of superconducting afterburner operation at SASE2 beamline of European XFEL," *Proc. SPIE 12581, X-Ray Free-Electron Lasers: Advances in Source Development and Instrumentation VI*, p. 1 258 105, 2023. doi:10.1117/12.2669177

[4] B. W. J. McNeil *et al.*, "Harmonic Lasing in a Free-Electron-Laser Amplifier," *Phys. Rev. Lett.*, vol. 96, p. 084 801, 2006. doi:10.1103/PhysRevLett.96.084801

[5] E. A. Schneidmiller and M. V. Yurkov, "Harmonic lasing in x-ray free electron lasers," *Phys. Rev. ST Accel. Beams*, vol. 15, p. 080 702, 2012. doi:10.1103/PhysRevSTAB.15.080702

[6] E. A. Schneidmiller, "Harmonic lasing at EuXFEL", presentation, Hamburg, Oct 2022.

[7] I. Nam *et al.*, "Soft X-ray harmonic lasing self-seeded free electron laser at Pohang Accelerator Laboratory X-ray free electron laser," *Appl. Phys. Lett.*, vol. 112, p. 213 506, 2018. doi:10.1063/1.5030443

[8] E. A. Schneidmiller *et al.*, "Observation of harmonic lasing in the Angstrom regime at European X-ray Free Electron Laser," *Phys. Rev. ST Accel. Beams*, vol. 24, p. 030 701, 2021. doi:10.1103/PhysRevAccelBeams.24.030701

[9] S. Liu *et al.*, "Preparing for high-repetition rate hard x-ray self-seeding at the European X-ray Free Electron Laser: Challenges and Opportunities," *Phys. Rev. Accel. Beams*, vol. 22, p. 060 704, 2019. doi:10.1103/PhysRevAccelBeams.22.060704

[10] S. Liu *et al.*, "Cascaded hard X-ray self-seeded free-electron laser at megahertz repetition rate," *Nat. Photonics*, vol. 17, pp. 984–991, 2023. doi:10.1038/s41566-023-01305-x

[11] https://henke.lbl.gov/optical_constants/ (last access: May 12, 2024).

[12] S. Reiche, "GENESIS 1.3: a fully 3D time-dependent FEL simulation code," *Nucl. Instrum. Meth. A*, vol. 429, pp. 243–248, 1999. doi:10.1016/S0168-9002(99)00114-X

[13] S. Reiche and C. Lechner, "Status of the time-dependent FEL code Genesis 1.3", presented at the 15th Int. Particle Accelerator Conf. (IPAC'24), Nashville, TN, USA, May 2024, paper WEPR58, this conference.

[14] Source Code of "Genesis 1.3", version 4: https://github.com/svenreiche/Genesis-1.3-Version4 (last access: May 12, 2024).

[15] B.E.A. Saleh and M.C. Teich, *Fundamentals of Photonics*, Wiley, Hoboken, NJ, USA (2007).